Eur Biophys J (2004) 33: 38–49
DOI 10.1007/s00249-003-0350-7

ARTICLE

**Ettore Bismuto · Roberto Nucci · Ferdinando Febbraio
Fabio Tanfani · Fabrizio Gentile · Raffaella Briante
Andrea Scirè · Enrico Bertoli · Pietro Amodeo**

Effects induced by mono- and divalent cations on protein regions responsible for thermal adaptation in β-glycosidase from *Sulfolobus solfataricus*

Received: 30 May 2003 / Accepted: 18 August 2003 / Published online: 15 October 2003
© EBSA 2003

Abstract The perturbation induced by mono- and divalent cations on the thermophilicity and thermostability of *Solfolobus solfataricus* β-glycosidase, a hyperthermophilic tetrameric enzyme, has been investigated by spectroscopic and computational simulation methods to ascertain the Hofmeister effects on two strategic protein regions identified previously. Specifically, (1) an extra segment (83–124), present only in the sequence of hyperthermophilic glycosidases and recognized as an important thermostability determinant for the enzyme structure; and (2) a restricted area of the subunit interface responsible for the quaternary structure maintenance. Mono- and divalent cations inhibit to a different extent the β-glycosidase activity, whose kinetic constants show an apparent competitive inhibition of the catalytic process that reflects the Hofmeister order. The thermostability is also affected by the nature and charge of the cations, reaching maximal effects for the case of Mg^{2+}. Fourier transform infrared spectroscopy has revealed very small changes in the protein secondary structure in the presence of the investigated cations at 20 °C, while large effects on the protein melting temperatures are observed. Computational analysis of the enzyme structure has identified negative patches on the accessible surface of the two identified regions. Following the Hofmeister series, cations weaken the existing electrostatic network that links the extra segment to the remaining protein matrix. In particular, the perturbing action of cations could involve the ionic pair interactions E107–R245 and E109–R185, thus leading to a local destructuring of the extra segment as a possible starting event for thermal destabilization. A detailed investigation of the electrostatic network at the A–C intermolecular interface of Sβgly after energy minimization suggests that cations could cause a strong attenuation of the ion pair interactions E474–K72 and D473–R402, with consequent partial dissociation of the tetrameric structure.

Keywords Cation effects · β-Glycosidase · Hofmeister series · Hyperthermophilic enzyme · Protein thermostability

Abbreviations *Amide I′* amide I band in a ^2H_2O medium · *EM* energy minimization · *ONPG* *o*-nitrophenyl-β-D-galactopyranoside · *S*βgly *Escherichia coli* expressed *Sulfolobus solfataricus* β-glycosidase

R. Nucci (✉) · F. Febbraio · R. Briante
Institute of Protein Biochemistry,
National Research Council,
Via Marconi 10, 80125 Naples, Italy
E-mail: nucci@ibpe.na.cnr.it
Tel.: +39-81-7257300
Fax: +39-81-7257300

E. Bismuto
Dipartimento di Biochimica e Biofisica, Seconda Università di Napoli, Via Costantinopoli 16,
80138 Napoli, Italy

F. Tanfani
Institute of Biochemistry,
Faculty of Sciences and INFM Ancona,
Università Politecnica delle Marche,
Via Ranieri, 60131 Ancona, Italy

A. Scirè · E. Bertoli
Institute of Biochemistry,
Faculty of Medicine and Surgery and INFM Ancona,
Università Politecnica delle Marche,
Via Ranieri, 60131 Ancona, Italy

F. Gentile
Centre of Endocrinology and Experimental Oncology,
National Research Council,
Via Pansini 5, 80131 Naples, Italy

P. Amodeo
Institute for Molecular Chemistry of Biological Interest (ICMIB),
National Research Council,
Comprensorio Olivetti, Edificio 70,
Via Campi Flegrei 34,
80078 Pozzuoli (Naples), Italy

Introduction

The proteins from hyperthermophilic organisms maintain their biologically active structure at temperatures

that are remarkably higher than the denaturation temperatures of their mesophilic counterparts (Jaenicke 1996; Jaenicke and Bohm 1998). However, the main question, namely which properties cause the increase in the denaturation temperature of thermostable proteins, is still under consideration (Karshikoff and Ladestein 2001). Recent studies on the experimental determination of the 3-D structures of particular hyperthermophilic proteins suggest an increase in ion pairs and/or hydrogen bonds as the principal determinants of the increased thermostability (Dao-Pin et al. 1991; Marqusee and Sauer 1994; Vogt et al. 1997). An analysis carried out on the structural differences among mesophilic, moderately and extremely thermophilic proteins (25 families) indicated an increase of about four extra ion pairs (within 4 Å) in a 300-residue protein from an organism with a T_{opt} of about 80 °C, in comparison with its mesophilic homologue with a T_{opt} of about 30 °C (Szilàgyi and Zavodszky 2000). On the other hand, some theoretical and experimental studies, most of them made at room temperature, have concluded that salt bridges usually destabilize, or at most slightly stabilize, the native state of the proteins (Sali et al. 1991; Sun et al. 1991; Hendsch and Tidor 1994; Waldburger et al. 1995). The supposed major reason for the low stability of a salt bridge at room temperature is that the association of two charged residues to form a salt bridge requires a large desolvation penalty, which is not fully compensated by favourable interactions between the salt bridge and the remaining matrix of the protein. At high temperatures, the decrease of the water dielectric constant markedly reduces this desolvation penalty, and, consequently, stabilizes the salt bridges (Elcock 1998; Karshikoff and Ladestein 2001).

Since it is generally well recognized that the ionic environment (water dielectric constant, ionic field, nature of ions, etc.) influences the properties of proteins in aqueous solution, a condition in which the net charge of a protein is compensated by an appropriate number of oppositely charged ions, the study of the effects induced by different ionic species seems to be meaningful. In fact this environment mimics biological conditions where ions can compete with salt bridges and intramolecular hydrogen bonds inside the protein. The main possible effects of ions on protein structure can consist of a non-specific screening (with consequent weakening) of inter- and intramolecular electrostatic interactions involving charged side chains (Pfeiffer et al. 1999), and the formation of specific local interactions among polar or charged groups of opposite charge.

This article focuses on the effects of ionic strength and mono- and divalent cations on the activity and thermal stability of the hyperthermophilic β-glycosidase from the extremophilic crenarchaeon *Sulfolobus solfataricus* to better understand the role of electrostatic charges on protein thermostability. β-Glycosidase is an homotetramer with $M_r = 240{,}000$ and is barely active at 30 °C, showing its maximum activity near 95 °C at pH 7.0; its thermostability analysis showed a $t_{1/2}$ of 85 h at 75 °C (Nucci et al. 1993). The protein structure evidences a typical α/β TIM barrel motif characteristic of proteins belonging to the glycosyl hydrolase family (Aguilar et al. 1997). The β-glycosidase enzyme from *Sulfolobus solfataricus* used in our investigation was expressed in the mesophilic host *Escherichia coli* (Sβgly) and demonstrated to possess the same structural and functional characteristics as the wild type (Febbraio et al. 1997). No direct experimental proof of the implication of the ion pairs and more generally of the electrostatic charge arrangement in the protein thermostability has been done so far. The enzymatic activity dependence on the mono- and divalent cation concentration as well as the thermostability as observed by Fourier transform infrared (FT-IR) techniques reflect the Hofmeister series (Neagu et al. 2001). Computer dynamic simulation evidences the presence of ion pairs as well as patches of negative charges localized in protein regions of strategic value for the thermostability and maintenance of the quaternary structure (Gentile et al. 2002; Bismuto et al. 2003).

Materials and methods

Materials

All chemicals used were of analytical grade from commercial sources. Centricon 30 centrifugal filter devices with YM-30 membranes were from Millipore (USA); deuterium oxide (99.9% ^2H_2O) was purchased from Aldrich. All the cations used were chloride salts. Homogeneous Sβgly was prepared according to Febbraio et al. (1997), and its concentration was estimated by UV measurements at 280 nm ($\epsilon = 9.5\times10^5$ cm^{-1} M^{-1}).

Sβgly kinetic analysis

The standard enzymatic assay was carried out on *o*-nitrophenyl-β-D-galactopyranoside (ONPG) as substrate at 75 °C, as previously described (Nucci et al. 1993). The enzymatic activity in the presence of K^+, Na^+, Li^+, Ba^{2+}, Ca^{2+} and Mg^{2+} was measured at each cation concentration in 20 mM Hepes buffer (pH 7.5), using 2.1 pmol of Sβgly and 2.8 mM ONPG as substrate in 1 mL final volume, at a temperature of 75 °C.

The kinetic constants of Sβgly were determined at the same ionic strength for mono-and divalent cations, and at a temperature of 60 °C in 20 mM Hepes buffer (pH 7.5), using ONPG as substrate in a concentration range from 0.1 to 36 mM. All the kinetic experiments were repeated several times and all the data were analysed with the program Grafit 3.0 (Erithacus Software) of R.J. Leatherbarrow. All the enzymatic assays were carried on in a thermostated Cary 1 spectrophotometer (Varian, Australia).

Sβgly thermal analysis

The dependence on temperature of the enzymatic activity for the different cations, in the absence and presence of 300 mM K^+ and 100 mM Mg^{2+}, was estimated by assaying enzyme aliquots of 4.1 pmol in 1 mL sample mixture containing 20 mM Hepes buffer (pH 7.5) and 2.8 mM ONPG as substrate, in the temperature range 25–90 °C. Thermal stability in the presence of the cations was measured by incubating 0.41 μM of the homogeneous enzyme in 20 mM Hepes buffer (pH 7.5) at 60, 70 and 80 °C at 300 mM K^+

and 100 mM Mg^{2+}, respectively. At time intervals, aliquots containing 4.1 pmol of enzyme were withdrawn from the incubation mixture and assayed at 75 °C under standard conditions.

IR spectra

Typically, 1–1.5 mg of protein dissolved in the same buffer used for its purification (0.1 M sodium phosphate, pH 7.0) were centrifuged in a Centricon 30 micro concentrator (Amicon) at 3000×*g* at 4 °C and concentrated into a volume of approximately 40 μL. The concentrated sample was washed with 300 μL of 20 mM Hepes buffer prepared in ^2H_2O (p^2H 7.5), or with 300 μL of the same buffer containing 100 mM Mg^{2+} or 300 mM K^+, and concentrated as described above. This procedure was repeated several times in order to completely replace the original buffer with the Hepes buffer. The washings took 24 h, which was the time of contact of the protein with the ^2H_2O medium prior to FT-IR analysis. In the last washing the protein sample was concentrated to a final volume of approximately 40 μL. The concentrated protein samples were placed in a thermostated Graseby Specac 20500 cell (Orpington, Kent, UK) fitted with CaF_2 windows and 25 μm Teflon spacers. FT-IR spectra were recorded by means of a Perkin-Elmer 1760-x Fourier transform infrared spectrometer using a deuterated triglycine sulfate detector and a normal Beer-Norton apodization function. At least 24 h previously, and during data acquisition, the spectrometer was continuously purged with dry air at a dew point of −40 °C. Spectra of buffers and samples were acquired at 2 cm^{-1} resolution under the same scanning and temperature conditions. Typically, 256 scans were averaged for each spectrum obtained at 20 °C, while 16 scans were taken for the spectra obtained at higher temperatures.

In the thermal denaturation experiments, the temperature was raised in 5 °C steps from 20 °C to 95 °C. Before spectrum acquisition, samples were maintained at the desired temperature for 6 min, which is the time necessary for the stabilization of the temperature inside the cell. Spectra were collected and processed using the "Spectrum" software from Perkin-Elmer. Second-derivative spectra were calculated over a 9-data-point range (9 cm^{-1}). The deconvoluted parameters were set with a gamma value of 2.5 and a smoothing length of 60.

CD spectroscopy

Near-UV CD spectroscopy was performed on Sβgly samples at a concentration of 2.05 μM in 20 mM Hepes buffer (pH 7.5) in the absence and presence of 300 mM K^+ and of 100 mM Mg^{2+} at temperatures of 20, 40, 60 and 70 °C. We used a J-710 spectropolarimeter (Jasco, Tokyo, Japan) calibrated by a standard solution of (+)-10-camphorsulfonic acid and equipped with a Neslab RTE-110 temperature-controlled liquid system (Neslab Instruments, Portsmouth, NH, USA). Photomultiplier absorbance did not exceed 500 V in the spectral region measured. All measurements were performed in 1.0 cm path length cuvettes (Helma, Jamaica, NY, USA) and under a 3 mL min^{-1} nitrogen flow. Before undergoing CD analyses, all samples were kept at the temperatures under study for 5 min in order to stabilize the temperature inside the cell.

Structure calculations

Sβgly modelled structures were refined by EM calculations using the AMBER 4.1 package (Weiner and Kollman 1981; Weiner et al. 1984, 1986), with the AMBER94 All-Atom parameterization (Cornell et al. 1995). EM calculations were performed in vacuo, with a distance-dependent dielectric constant $\epsilon = r$ to roughly reproduce solvation effects. In addition, a reduction from 1 to 0.2 of the absolute value of the total charge was used for acid and basic residues and for terminal NH_3^+ and COO^- groups, to avoid over stabilization of H-bonds and salt bridges. This whole procedure should prevent from obtaining artificially compact structures, with overwhelming patterns of polar interactions acting as the driving forces for both intra- and intermolecular interactions. Final refinement steps were run in a periodic water box. A 8 Å cut-off for no-bonded interactions was used in all the calculations. The resulting structures were analysed with the MOLMOL (Koradi et al. 1996) program, which was also used to produce all the molecular plots.

The NACCESS program (Hubbard and Thornton 1993) was used for calculation of solvent accessibilities and buried areas. In this analysis the standard values of the atomic van der Waals radii, included in the program, were used with a spherical probe radius of 1.4 Å. The cartesian coordinates of the hydrogen atoms, missing in the reference crystallographic structure, were calculated with the HBPLUS program (McDonald and Thornton 1994), also used to perform further H-bond analysis.

Results

Sβgly kinetic analysis

Enzyme activity can be regarded as the most sensitive probe for studying the changes in enzyme conformation during various treatments, as it reflects subtle readjustment at the active site, allowing very small conformational variations of an enzyme structure to be detected. Concerning this, we have used some chemical perturbants such as ionic strength and cations to monitor the effects on protein function and structure.

Figure 1A shows the Sβgly activity (%) dependence on KCl concentrations in 20 mM Hepes buffer (pH 7.5)

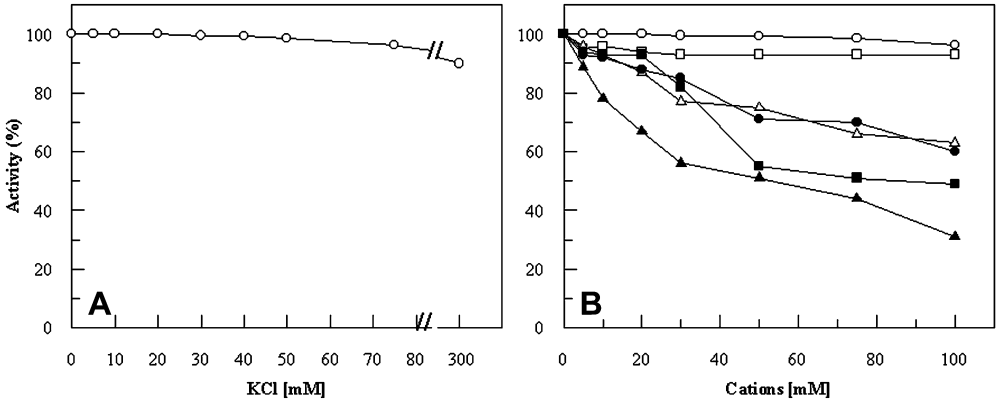

Fig. 1 A Effect on Sβgly activity in 20 mM Hepes buffer (pH 7.5) as a function of different KCl concentrations in the range 1–300 mM (ionic strength in the range 0.00–0.32). **B** Effect on Sβgly activity of different cation concentrations in the range from 0 to 100 mM K^+ (*open circles*), Na^+ (*open squares*), Li^+ (*open triangles*), Ba^{2+} (*closed circles*), Ca^{2+} (*closed squares*), Mg^{2+} (*closed triangles*). All the cations have Cl^- as the counter ion

at 75 °C in the range 0–300 mM. The enzymatic activity is scarcely affected by the KCl ionic strength. Figure 1B shows the dependence of enzymatic activity (%) for other mono- and divalent cations. The inhibition exerted by the cations varies according to the following order: $K^+ < Na^+ < Li^+, Ba^{2+} < Ca^{2+} < Mg^{2+}$, with an indication that the inhibition is not only correlated to the absolute values of the ion charges but also increases with the decreasing ion radius; moreover, the sequence follows the Hofmeister series order (Lo Nostro et al. 2002). Specifically, K^+ and Mg^{2+} affect the enzyme activity by a significantly different extent: 96% and 31% of residual activity was measured at 100 mM concentration of each cation, respectively.

A more extensive kinetic investigation was performed by evaluating the kinetic constants at two different ion concentrations, i.e. 150 mM and 300 mM for K^+ and 50 mM and 100 mM for Mg^{2+}, respectively. Table 1 summarizes these kinetic data. In connection with this, we report K_M, K_{cat} and K_i values at a temperature of 60 °C to avoid all possible denaturing effects induced by cation addition observable over 80 °C. The kinetic data indicate a decrease of enzyme affinity for the substrate ONPG caused by each of the two cations, with significant higher values of apparent K_M in presence of Mg^{2+}. Concerning the turnover numbers (K_{cat}), they appear essentially unmodified with a consequent lost of enzyme specificity (K_{cat}/K_M) for the tested substrate. Linear plots of reciprocal velocities versus reciprocal substrate concentrations, in the presence and absence of cations, point out an apparent competitive inhibition caused by these cations. In agreement with this mechanism, the K_i values are calculated by the equation:

$$K_i = \frac{i}{\frac{K_P}{K_M} - 1} \quad (1)$$

where i is the inhibitor concentration and K_P is the Michaelis constant in the presence of inhibitor. For K^+, the K_i is higher than 200 mM (more than 200 times that of the K_M of the enzyme without K^+), according with its very low degree of inhibition, whereas in the presence of 50 and 100 mM Mg^{2+}, K_i values of 13 and 12 mM are observed, respectively, in agreement with its higher degree of inhibition (Table 1). These values are about 15 times higher than the K_M value for the substrate ONPG (0.84 mM) at 60 °C for the enzyme in the absence of Mg^{2+}. The apparent competitive inhibition noted in the presence of K^+ and Mg^{2+} on the Sβgly activity correlates well with an increasing value of the cation charge density that we can interpret as due to a stronger disturbing effect in the Sβgly active site by cations, according to $Mg^{2+} > K^+$.

Sβgly thermal analysis

To compare the Sβgly thermal activity in the absence and presence of K^+ and Mg^{2+}, standard enzymatic assays at different temperatures were carried out. The temperature versus activity profiles were different (Fig. 2A), displaying a slight apparent competitive inhibition by K^+ at lower temperature, overcome by the temperature increase. In the presence of Mg^{2+} a decrease in absolute activity, more evident at high temperature, was observed. On the other hand, if we analyse the trend of activity increase, reported in %, against temperature (insert Fig. 2A), comparable values in the absence and presence of Mg^{2+} are obtained, suggesting that enzyme thermal denaturation under the experimental conditions of the assay (1 min) can be excluded, whereas the loss in absolute activity is related to the apparent competitive inhibition (see previous section).

The thermal stability profiles (Fig. 2B–D), carried out at different temperatures (60, 70 and 80 °C) for the enzyme in the absence and in the presence of 300 mM K^+ and 100 mM Mg^{2+}, showed that K^+ has a significant effect on the thermal stability only at 80 °C (see Fig. 2D). Contrarily, the enzyme in the presence of Mg^{2+} displays about 10% of inactivation during the first 5 h of incubation at 60 °C, whereas at 70 °C and 80 °C a more pronounced inactivation was observable, with a $t_{1/2}$ of 4 h at 80 °C (Fig. 2B–D) and with a dramatic lost of thermostability, this being much lower than that of the protein in the absence of this cation ($t_{1/2}$ of 85 h at 75 °C). All functional data support a strong effect of Mg^{2+} by leading to a less thermophilic and a less thermostable enzyme, characterized by structural damage widespread to other protein areas, different from the catalytic site, but involved in protein thermal activation and stabilization at high temperatures.

FT-IR spectroscopy: secondary structure content and thermal stability of Sβgly in the absence and in the presence of K^+ and Mg^{2+}

An IR spectroscopic study, in order to evaluate the possible cations' effect on protein secondary structure content and on its thermal stability, was carried out. Figure 3 shows the second-derivative spectrum

Table 1 Kinetic constants of Sβgly in the absence and in the presence of K^+ and Mg^{2+} at the indicated concentrations

	[Cation] (mM)	K_M (mM)	K_{cat} (s^{-1})	K_{cat}/K_M (s^{-1} mM^{-1})	K_i (mM)
Sβgly	–	0.84 ± 0.07	445.6 ± 9.0	530.4	–
+ KCl	150	1.37 ± 0.12	477.0 ± 10.0	348.2	> 200
+ KCl	300	1.74 ± 0.15	432.8 ± 10.0	248.7	> 200
+ $MgCl_2$	50	4.07 ± 0.07	472.0 ± 2.4	115.9	13
+ $MgCl_2$	100	7.78 ± 0.36	450.0 ± 7.6	57.8	12

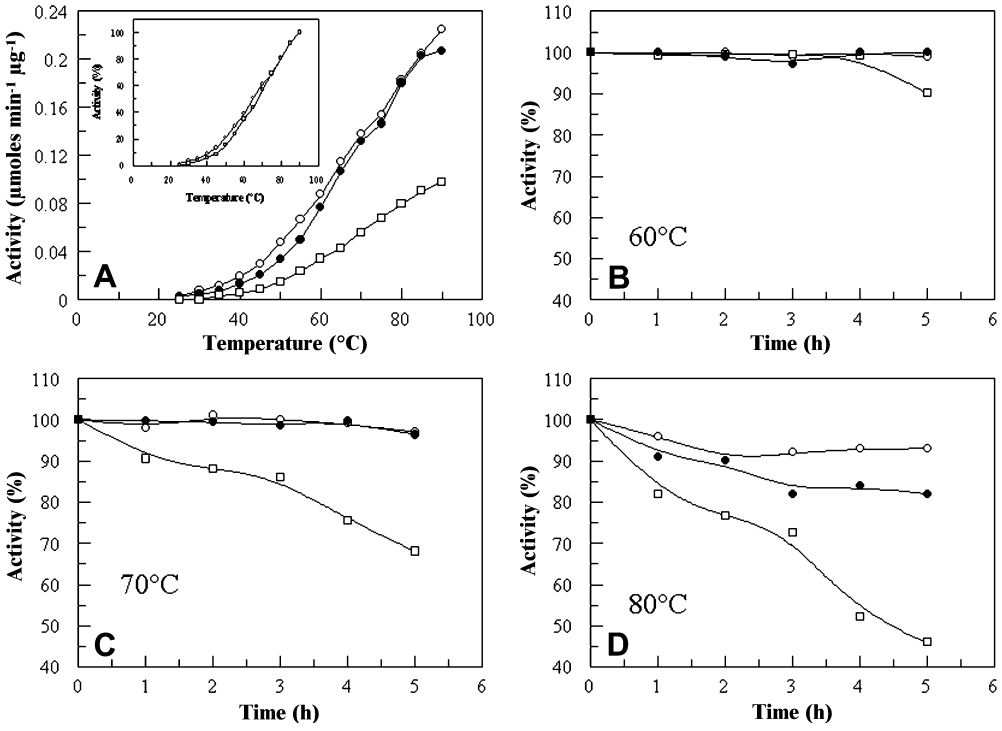

Fig. 2 A Thermal activity of Sβgly in the temperature range 25–90 °C: enzyme in 20 mM Hepes buffer (pH 7.5) (*open circles*), enzyme in the presence of 300 mM K^+ (*closed circles*), enzyme in the presence of 100 mM Mg^{2+} (*open squares*). *Insert*: plot of enzymatic activity in % against temperature in the range 25–90 °C in the absence (*open circles*) and in the presence of 100 mM Mg^{2+} (*open squares*). **B–D** Thermal stability of Sβgly: enzyme alone (*open circles*), enzyme in the presence of 300 mM K^+ (*closed circles*), enzyme in the presence of 100 mM Mg^{2+} (*open squares*), at temperatures of 60 °C (*continuous line*), 70 °C (*dashed line*) and 80 °C (*dotted line*)

(spectrum A) of recombinant β-glycosidase in 20 mM Hepes (p^2H 7.5). The resolution-enhanced spectra show the amide I′ band (1700–1600 cm^{-1}) components as well-resolved peaks or as shoulders. Each band or shoulder is due to a particular secondary structure or to amino acid side-chain absorption (Arrondo et al. 1993; Chirgadze et al. 1975). The 1654.9, 1644.3 and 1636.5 cm^{-1} bands are due to α-helices, unordered structures and β-sheets, respectively (Arrondo et al. 1993). β-Strands particularly exposed to the solvent are revealed by the 1627 cm^{-1} shoulder (Arrondo et al. 1988; Jackson and Mantsch 1991). The 1683 cm^{-1} band could contain information on β-sheets and/or turns since theoretical (Krimm and Bandekar 1986) and empirical (Byler and Susi 1986) studies on proteins show that both structures can absorb in this region. The 1666.8 cm^{-1} peak is due to turns (Byler and Susi 1986) while the peaks below 1615 cm^{-1} are due to amino acid side-chain absorption (Chirgadze et al. 1975), except the 1547.6 cm^{-1} band which represents residual amide II band absorption (Osborne and Nabedryk-Viala 1982). This last band is the result of uncompleted $^1H \rightarrow {}^2H$ exchange and indicates that the solvent (^2H_2O) cannot reach all the protein's segments at 20 °C (Osborne and Nabedryk-Viala 1982).

Figure 3 (spectra B and C) shows the effect of Mg^{2+} and K^+ ions, respectively, on the second-derivative spectra of Sβgly at 20 °C. In all cases, a small upshift in wavenumber of the β-sheet band can be observed. This result suggests that the above ions allow a lower access of the solvent (^2H_2O) to the β-sheets, since the higher the $^1H \rightarrow {}^2H$ exchange, the lower wavenumber band position (D'Auria et al. 1999). In the presence of Mg^{2+}, this effect should concern at least part of the β-sheets, since the increase in the 1627 cm^{-1} band intensity suggests that the ion leads some β-strands to be more exposed to the solvent (spectrum B). Any difference is observed in the position of the α-helix band in the presence of cations. Second-derivative spectra also show small differences in the band intensities that could be enhanced by considering the difference spectra obtained using both second-derivative (continuous lines) or deconvoluted (dashed lines) spectra (inset B) (Umemura et al. 1980; Paolini et al. 1999; Pedone et al. 2003). Specifically, these spectra were obtained by subtracting the spectrum of Sβgly in the presence of Mg^{2+} or K^+ (B, C) from the spectrum in their absence (A). The similarity between the second-derivative and deconvoluted difference spectra supports the finding that cations induce small differences in the components of the amide I′ band. In particular, in the presence of K^+ the α-helix band intensity (1654.2 cm^{-1}) slightly increased whilst in the presence of Mg^{2+} the intensities of the bands close to 1627 cm^{-1} (exposed β-strands) and 1646 cm^{-1} (unordered structures) increased (see inset B). Other changes in the second-derivative spectra, induced by the above cations, can be observed close to 1685 cm^{-1} and in the region of β-sheet absorption.

All these data suggest that the above ions may induce very tiny changes in the secondary structure of β-glycosidase and that three-dimensional organizational changes might be also induced by Mg^{2+} as a consequence of the increase in exposed β-strands. According to the crystallographic coordinates of the protein, tyrosines that are more solvent exposed are present in β-strands, as well as in α-helices and random structures. It is interesting to underline that about half of these more exposed Tyr residues are available at subunit interfaces.

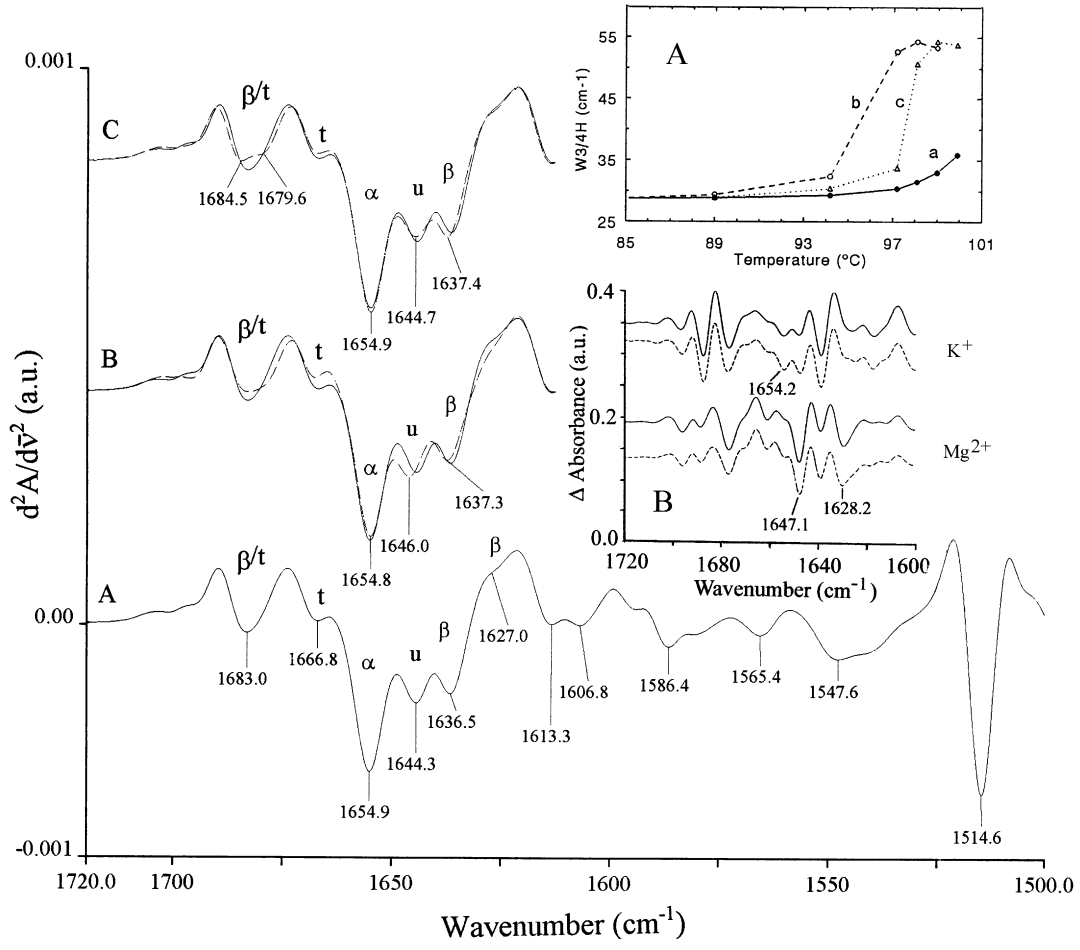

Fig. 3A–C *Main figure*: FT-IR second-derivative spectra of recombinant β-glycosidase in the absence (control) and in the presence of different metal ions at 20 °C and p^{2}H 7.5. The *continuous line* in spectra **A**, **B** and **C** represents the control (the protein in the presence of 20 mM Hepes, p^{2}H 7.5). The *dashed line* in **B** and **C** represents the second-derivative spectra of β-glycosidase in the presence of 20 mM Hepes/100 mM Mg^{2+} and 20 mM Hepes/300 mM K^+, respectively. The symbols α, β, *t* and *u* stand for α-helix, β-sheet, turns and unordered structures, respectively. The spectra were obtained from original absorbance spectra normalized at the amide I′ band area. *Inset A*: thermal denaturation curves of the protein in the absence (*continuous line a*, *full circles*) and in the presence of 300 mM K^+ (*dotted line c*, *open triangles*) and 100 mM Mg^{2+} (*dashed line b*, *open circles*). To obtain the curves, the amide I′ bandwidth of the absorbance spectra was monitored, at 3/4 of amide I′ band height (W3/4H), as a function of the temperature. *Inset B*: difference spectra at 20 °C, obtained by subtracting the spectrum of Sβgly in the presence of 300 mM K^+ (K^+) or 100 mM Mg^{2+} (Mg^{2+}) from the control spectrum. *Continuous* and *dashed lines* represent second-derivative and deconvoluted difference spectra, respectively. The two spectra on the top of the inset are the difference spectra that were normalized to 0.1 Δ absorbance value

In order to follow the thermal denaturation of protein samples, the plots of the amide I′ bandwidth versus temperature (Tanfani et al. 1998) are shown in inset A of Fig. 3. The curves are relative to: Sβgly in Hepes buffer (curve a), with an indication of $T_m > 99.9$ °C; Sβgly in Hepes buffer in the presence of 300 mM K^+ with $T_m = 97.5$ °C (curve c); and Sβgly in Hepes buffer in the presence of 100 mM Mg^{2+} (curve b) with $T_m = 95.5$ °C. The results indicate a significant difference in the onset of the denaturation temperature in the presence of Mg^{2+} in comparison to that of the protein in the presence of K^+ and even more to that observed in the absence of inorganic cations.

The second-derivative spectrum of Sβgly in Hepes buffer shows that, at 20 °C, the $^1H \rightarrow {}^2H$ exchange in the protein was not complete. Similar results were obtained with the protein in the presence of Mg^{2+} or K^+. At temperatures higher than 20 °C the $^1H \rightarrow {}^2H$ exchange increased and reached a maximum when the protein unfolded. As an example, Fig. 4 shows the original absorbance spectra of Sβgly in the presence of K^+ recorded at different temperatures. With the increase of the temperature, the intensity, the position and the width of the amide I′ band remains almost constant until 89 °C. Then, owing to protein denaturation, the amide I′ band intensity decreases and the band broadens and shifts. In particular, protein aggregation, brought about by denaturation of the polypeptide chains, parallels the unfolding of the protein. This is seen by the appearance of new peaks close to 1620 and 1680 cm^{-1} (Tanfani et al. 1998 and references therein). The appearance of these new bands contributes significantly to the increase of the amide I′ bandwidth. Figure 4 shows also that, at temperatures

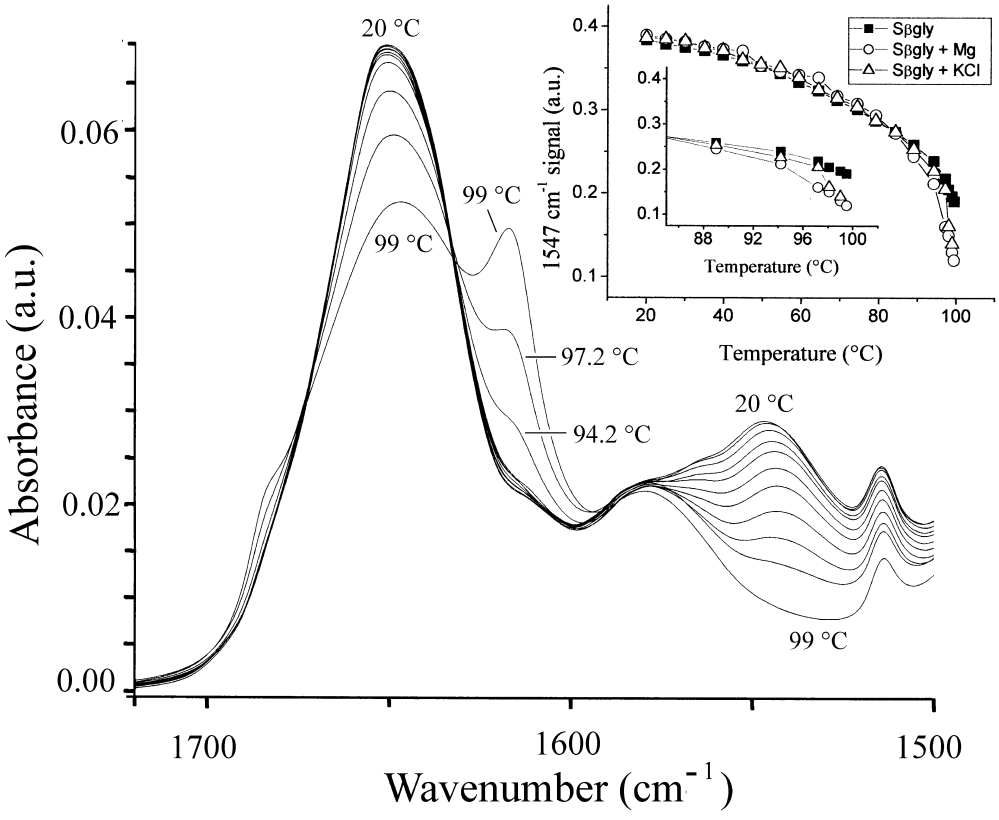

Fig. 4 *Main figure*: original absorbance spectra of Sβgly in the presence of 300 mM K^+ at p^{2}H 7.5. The displayed spectra were obtained at 20, 30, 39.8, 49.5, 59.3, 69.2, 79.2, 89.0, 94.2, 97.2 and 99.0 °C. *Inset*: signal of the residual amide II band intensity (1547 cm^{-1}) as a function of the temperature. The intensity of the amide II band was calculated after normalization of the amide I′ band intensity to 1.0 absorbance value. In the inset, an expanded view of the graph (88–100 °C region) is shown

higher than 20 °C, the residual amide II band intensity decreases, a phenomenon due to a further $^1H \rightarrow {}^2H$ exchange. The inset reports the plot of the intensity of the residual amide II band as a function of temperature. All protein samples display a similar ability to exchange amide hydrogens with deuterium. The highest tendency of $^1H \rightarrow {}^2H$ exchange is found in the range of temperatures in which protein denaturation occurs (88–99.5 °C), as shown by the main figure and by the change in the slope of the curves in the inset. However, between 88 and 99.5 °C the $^1H \rightarrow {}^2H$ exchange in the three protein samples is significantly different, following the order Sβgly + Mg^{2+} > Sβgly + K^+ > Sβgly (see expanded view in the inset). In particular, the lower the thermal stability, the higher the $^1H \rightarrow {}^2H$ exchange in the 88–99.5 °C temperature range (see inset A in Fig. 4).

CD in the near UV

Near-UV CD spectroscopy experiments were performed in the 250–300 nm region, to detect the effects of K^+ (300 mM) and Mg^{2+} (100 mM) on the Sβgly amino acid side chains, from 20 °C to 70 °C. Higher temperatures are forbidden for protein aggregation phenomena, at these concentrations.

The near-UV CD spectra of the protein in the absence and in the presence of Mg^{2+} or K^+, respectively, at 70 °C, are shown in Fig. 5. The near-CD signal is mainly produced by the interactions of aromatic residues with specific side chains forming its surroundings (Strickland 1974). Mg^{2+} seems to strengthen these interactions more than K^+, although the observed differences in the CD spectra are quite small.

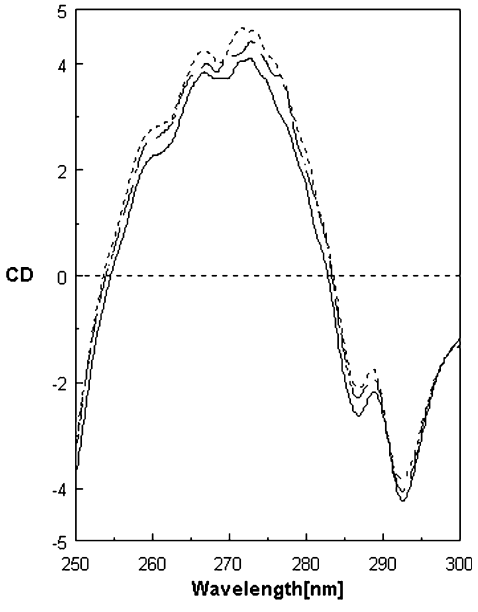

Fig. 5 Near-UV CD spectra of Sβgly in the absence (*continuous line*) and in the presence of K^+ (*dashed line*) and Mg^{2+} (*dotted line*), at 70 °C

Computational analysis

The net negative charge of Sβgly, calculated by amino acid composition, amounts to −36 at pH 7.0. The energy minimization of the Sβgly structure starting from the crystallographic coordinates (as reported in Material and methods) allows the evaluation of the electrostatic surface bordering the protein matrix.

The analysis of the distribution of negatively charged residues in the tetramer shows that patches of Asp and Glu residues exist on the surface, as well as in internal cavities corresponding to the active sites (Fig. 6a–c). In particular, the strong negative electrostatic field surrounding the channel leading to the active site is expected to promote the competitive inhibition driven by cations. The bottom of the active site also exhibits a large negatively charged surface, able to interact directly with positive ions as well as to promote their interaction with other negatively charged key residues in the active site (Fig. 6d). By clustering negatively charged residues in sets where the distance of one member from at least one other member of the set is less than 5 Å, six different patches formed by more than three residues are identified in each monomer (Table 2; Fig. 6e–g).

By using a different number of asterisks, the degree of solvent accessibility is indicated. Interestingly, three patches (2, 5 and 6) out of the six correspond to protein regions diverging appreciably from those observed in mesophilic homologues of this protein when structural alignment is performed within this class of protein (Bismuto et al. 2003). Patch 2 is inside the extra segment present only in hyperthermophilic proteins. The other two of these non-conserved regions (5, 6) are involved in an inter-monomer interface of Sβgly, whose importance in determining the stabilization of the A–C dimer chains of the crystal structure by a network of salt bridges, mediated by the solvent, has been recently published (Gentile et al. 2002). Concerning the other three patches, we can observe that: in patch (1), only one of the six involved residues is not conserved in structural alignment; the small (3) patch includes only structurally conserved residues and the alignment with the other reference structures in this region is rather poor. Patch 4 corresponds to a short α-helical segment composed of four conserved and four non-conserved residues.

Table 3 gives the inter- and intra-electrostatic interactions among charged close residues at a distance less than 5 Å in both the above-evidenced protein regions. Specifically, making reference to negative patch 2 of Table 2, we note that the non-conserved E112, E114 and D104 are involved in three intra-segment attractive interactions (E112–K116, E114–K116, D104–K102). Further contribution is given by the polar interaction Q96–N97. The non-conserved E107, E109, E112 and E114 are involved in four repulsive interactions (E107–E109, E109–E114, E112–E114, E114–D119). Concerning the extra segment–remaining structure attractive interactions, the destabilizing effect by cations may involve the three amino acid residues D104, E107 and E109, as present in the three ion pairs D104–R300, E107–R245 and E109–R185, whereas polar interactions are contributed by Q96–Y181 and N97–Y181. In the negative patch 5 of Table 2, the non-conserved D358 and D385 of the inter-monomeric interface A–C are capable of water-mediated intra- and inter-repulsive interactions, whereas the non-conserved D473 and E474 of the negative patch 6 are involved in productive electrostatic interactions which bind the inter-monomeric interface A–C through ion pairs D473 (monomer A)–R452 (monomer C) and E474 (monomer A)–K72 (monomer C).

Discussion

The results given in this article suggest that metal ions such as K^+ and Mg^{2+} affect the thermal stability of Sβgly. On the other hand, resolution-enhanced and difference spectra suggest that the cations may induce very tiny changes in the secondary structure of the protein and suggest an increased exposure of β-strands to the solvent in the presence of Mg^{2+} ions. The lower melting temperature (T_m) observed in the presence of the cations may be associated with the destabilization of salt bridges that, at high temperatures, due to the decrease of the water dielectric constant, are particularly important for protein stability (Elcock 1998; Karshikoff and Ladestein 2001). In turn, the destabilization of the protein structure induced an increase in the rate of $^1H \rightarrow {}^2H$ exchange in the 88–99.5 °C temperature range, as a consequence of protein denaturation. It is interesting to note that the higher the destabilization effect ($Mg^{2+} > K^+$), or the lower the T_m ($S\beta gly + Mg^{2+} < S\beta gly + K^+$), the higher the increase of the rate of $^1H \rightarrow {}^2H$ exchange in the 88–99.5 °C temperature range. The anticipated thermal denaturation of the protein could be attributed essentially to at least two effects:

1. Formation of non-productive ion pairs between negatively charged amino acid residues and the investigated cations, by preventing formation of the right ion pairs believed to be strategic for its thermal stabilization. This negative consequence is not fully compensated by the cation's weakness of the repulsive electrostatic force present in the enzyme molecule whose net negative charge amounts to −36 at neutral pH.
2. According to the Hofmeister series, Mg^{2+} is more strongly hydrated than K^+, thus causing a stronger perturbation of the hydrogen bond network of the aqueous solvent surrounding the protein matrix.

Recently, Honig's group, by comparing four different hyperthermophilic proteins with their mesophilic homologues, have shown that electrostatic interactions are more favourable in hyperthermophilic proteins. They suggest that the key feature is not ion pair

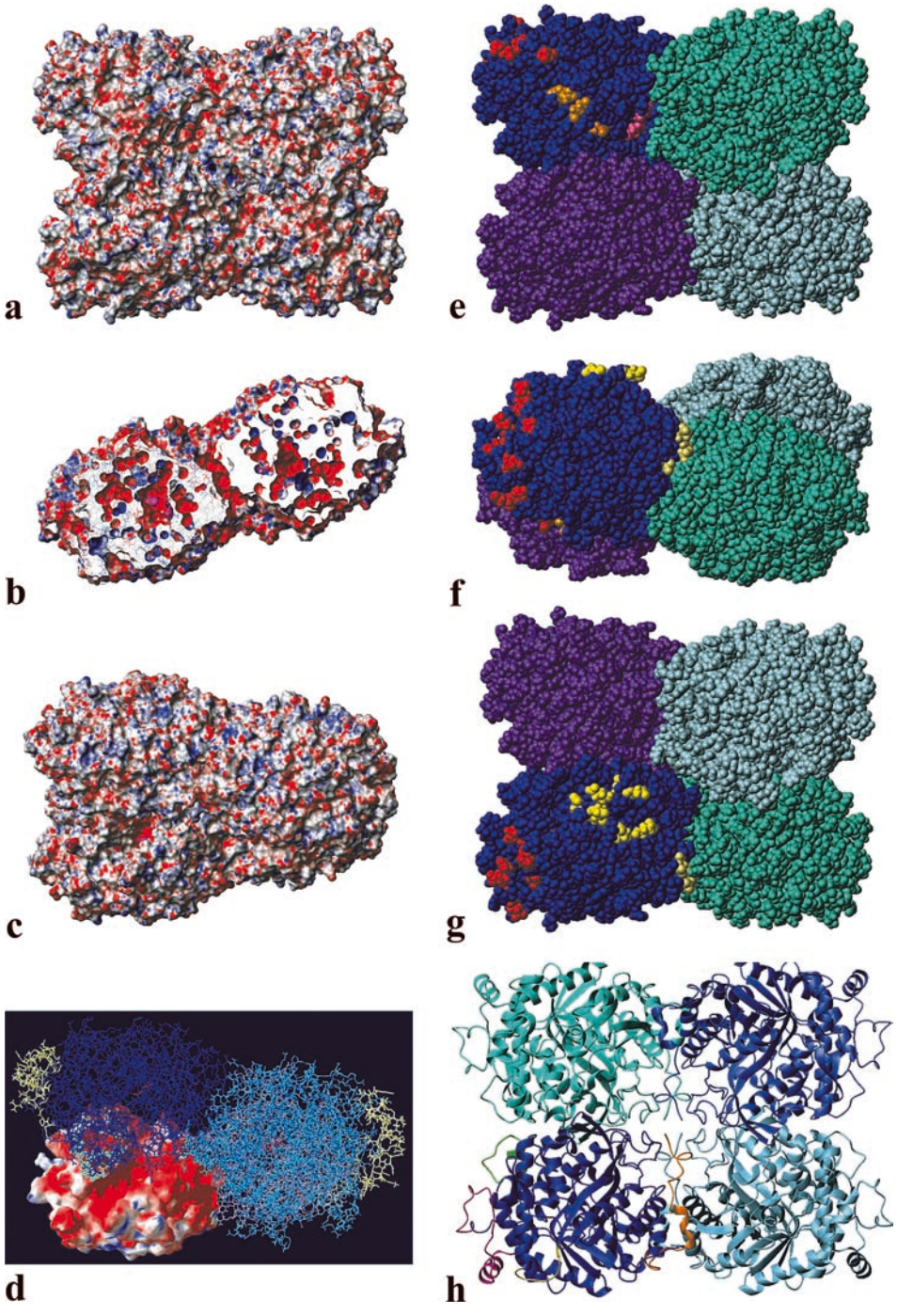

networks, but the optimum placement of the charged groups within the protein structure. In other words, the electrostatic interactions are optimized by avoiding repulsive charge–charge interactions in proteins: on average there are four attractive ion pairs but only one repulsive pair per 100 residues (Pace 2000).

Our functional, spectroscopic and computational results support the hypothesis that a local destabilizing action of cations on protein ion pairs at high temperatures may arise both by the breaking of properly placed charge–charge interactions in the structure or by perturbation in the solvent organization, according the Hofmeister series, that weakens the network of interactions with the enclosed protein surface, causing an anticipated thermal denaturation. The presence of negative charge clusters has been indicated by computational analysis showing six patches (Table 2), three of which are localized in previously identified regions as determinants for thermostability and quaternary arrangement of the Sβgly structure. Specifically, patch 2 corresponds to a long α-helical insertion bulging out each monomer in comparison with aligned mesophilic proteins (Fig. 5d and h); the strategic relevance of this

◄

Fig. 6a–h Graphical representations of the crystal structure of Sβgly. In **a**–**c** the projection of the electrostatic potential on the accessible surface is shown. *Red*, *blue* and *white regions* correspond to negative, positive and neutral potential values, respectively. Models **b** and **c** have been obtained by 90° and 65° rotations about the *x* (horizontal) axis of the orientation shown in **a**, respectively. Model **b** represents a section of the tetramer, providing a view of the active site of two monomers. The side chain of the catalytic Glu387 residue, in the monomer corresponding to the A chain of the crystal structure, is shown in *magenta space fill representation* in **b** and **c**. Model **d** shows a view of the electrostatic potential of a single monomer, in the same orientation as **b**, with Glu387 colored in *yellow*. The other monomers are drawn with a *stick representation* in different shades of *blue*, except for residues belonging to the non-conserved region Pro91–Asp119 in *yellow* and for Glu387 in *magenta*. Models **e**–**g** show three views of the protein van der Waals surface on which the patches of negatively charged residues described in Table 2 are indicated by colors. Different shades of *blue* are used for generic residues in the four monomers, while the Asp and Glu residues belonging to the 1–6 patches (Table 2) in the D monomer of the crystal structure are colored in *orange*, *red*, *red-orange*, *light yellow*, *pink* and *yellow*, respectively. Model **e** corresponds to the same view as **a**, while **f** and **g** have been obtained from **e** by 90° and 180° rotations about the *x* axis. Model **h** shows a *ribbon representation* of the tetramer, where the low-similarity regions identified in the structural alignment analysis are indicated (Bismuto et al. 2003). Different shades of *blue* are used for the four monomers, while low-similarity regions in the A chain of the crystal structure are represented with *magenta*, *green*, *yellow* and *orange ribbons*

structural element for β-glycosidase thermostability has been reported in a recent article (Bismuto et al. 2003) in which single mutations caused changes in the structural and dynamic properties of the protein with a simultaneous loss of its thermostability. The examination of the minimized Sβgly structure has allowed us to identify a complex network of ionic interactions among charged residues of extra segments and among themselves and charged residues belonging to the remaining protein matrix. Three out of nine inter-attractive interactions linking opposed charged groups (E107–R245, E109–R185, D104–R300) are solvent exposed and potential targets for cation weakness of productive interactions (Table 3). The residues at the interfaces between adjacent monomers in the Sβgly tetramer originate an overall negative electrostatic field on the protein surface surrounding the interfaces A–C (Fig. 5h). Specifically,

Table 2 Negatively charged surface patches on the tetramer

Patch	Negatively charged residues[a]
1	E20(*), E27(****), **D28**(*), D51(***), E54(***), E83(*)
2	**D104**(***), **E107**(****), **E109**(****), **E112**(****), **E114**(*)
3	**D119**(**), **E120**(****), D125(****), D248(***), D308(****), D309(**), D195(***), D196(****), D199(***), E200(*)
4	D272(****),**D274**(*),**E276**(****),**E279**(****), E282(*), **D284**(****), E366(****), D370(***)
5	**D358**(***), D392(*), **D393**(***), **D395**(*), D429(*)
6	E464(**),**D473**(****),**E474**(***),**E476**(***)

[a]Residues in bold are not conserved in structural alignments with homologous mesophilic proteins (see text for details). The asterisks in parentheses indicate the surface accessibility of the residues (*: < 5%; **: 5–10%; ***: 10–20%; ****: > 20%)

Table 3 Electrostatic interactions among amino acid residues in the extra segment and at the A–C monomeric interface. The interacting residues were obtained by surrounding the mass centre of each residue with a sphere of 4 Å radius

Interactions	Attractive	Repulsive	Polar
Intra–extra segment	D99–K102 D99–E109 E100–K102 K102–D104 E112–K116 E114–K116 K116–E120 R117–E120	D99–E100 E107–E109 E109–E114 E112–E114 E114–D119 K116–R117 D119–E120	Q96–N97 (2.37)
Intra–remaining structure	K124–D125 R178–E182 E182–R185 R185–K193 K193–D195 K193–D196 R245–D248 R245–D309 R307–D309	K124–K193 R245–R307 R300–R307	S176–T177 (2.25) Q103–T237 (2.87)
Extra segment–remaining structure	D99–R178 E100–R178 D104–R300 D104–R307 E107–R245 E109–R185 E114–R185 D119–K193 D119–K124		Q96–Y181 N97–Y181
Inter-monomeric interface A–C[a]	R452 (A)–D473 (C) D473 (A)–R452 (C) E474 (A)–K72 (C) R463–E464 (H_2O)	D358–D392–(H_2O) R488 (A)–K485 (C) D395 (A)–D395 (C)–(H_2O)	

[a](A) and (C) indicate the corresponding monomers of Sβgly

D473 (monomer A)–R452 (monomer C) and E474 (monomer A)–K72 (monomer C) are two inter-attractive interactions, solvent exposed, which can be disturbed by cations. The hyperthermophilic β-glycosidase from *S. solfataricus* is characterized by a higher number of charged and polar amino acid residues on its surface in comparison with mesophilic ones (Fukuchi and Nishikawa 2001); moreover, Sβgly contains nearly twice as many ionic groups involved in ion pairs (Aguilar et al. 1997). Conversely, the observed stabilization induced by monovalent/divalent cations with negatively charged moieties present in some mesophilic proteins such as glucose oxidase, having a strong negative net charge (−77 at neutral pH), can be explained as a compensation effect for the shortage of basic residues in the enzyme structure. Therefore, the cations act mainly by weakening the repulsive electrostatic force among negative clusters present in the protein surface, thus favouring compactness of the enzyme's conformation (Ahmad et al. 2001; Akhtar et al. 2002).

Acknowledgements This work was supported by a grant from the PRIN99 and PRIN01 project (F.T., E.B.) and by a grant from the National Research Council (Italy).

References

Aguilar CF, Sanderson I, Moracci M, Ciaramella M, Nucci R, Rossi M, Pear LH (1997) Crystal structure of the β-glycosidase from the hyperthermophilic archaeon *Sulfolobus solfataricus*: resilience as a key factor in thermostability. J Mol Biol 271:789–802

Ahmad A, Akhtar MS, Bhakuni V (2001) Monovalent cation induced conformational change in glucose oxidase leading to stabilization of the enzyme. Biochemistry 40:1945–1955

Akhtar MS, Ahmad A, Bhakuni V (2002) Divalent cation induced changes in structural properties of the dimeric enzyme glucose oxidase: dual effect of dimer stabilization and dissociation with loss of cooperative interactions in enzyme monomer. Biochemistry 41:7142–7149

Arrondo JLR, Young NM, Mantsch HH (1988) The solution structure of concanavalin A probed by FT-IR spectroscopy. Biochim Biophys Acta 952:261–268

Arrondo JLR, Muga A, Castresana J, Goni FM (1993) Quantitative studies of the structure of proteins in solutions by Fourier-transform infrared spectroscopy. Prog Biophys Mol Biol 59: 23–56

Bismuto E, Febbraio F, Limongelli S, Briante R, Nucci R (2003) Dynamic fluorescence studies of beta-glycosidase mutants from *Sulfolobus solfataricus*. Effects of single mutations on protein thermostability. Proteins 51:10–20

Byler DM, Susi H (1986) Examination of the secondary structure of proteins by deconvolved FTIR spectra. Biopolymers 25:469–487

Chirgadze YN, Fedorow OW, Trushina NP (1975) Estimation of amino acid residue side-chain absorption in the infrared spectra of protein solutions in heavy water. Biopolymers 14:679–694

Cornell WD, Cieplak P, Bayly CI, Gould IR, Merz KM Jr, Ferguson DM, Spellmeyer DC, Fox T, Caldwell JW, Kollman PA (1995) A second generation force field for the simulation of proteins and nucleic acids. J Am Chem Soc 117:5179–5197

Dao-Pin S, Sauer U, Nicholson H, Matthews B (1991) Contributions of engineered surface salt bridges to the stability of T4 lysozyme determined by directed mutagenesis. Biochemistry 30:7142–7153

D'Auria S, Nucci R, Rossi M, Bertoli E, Tanfani F, Gryczynski I, Malak H, Lakowicz JR (1999) β-Glycosidase from the hyperethermophilic Archaeon *Sulfolobus solfataricus*: structure and activity in the presence of alchols. J Biochem (Tokyo) 126:545–552

Elcock AH (1998) The stability of salt bridges at high temperatures: implications for hyperthermophilic proteins. J Mol Biol 284:489–502

Febbraio F, Barone R, D'Auria S, Rossi M, Nucci R, Piccialli G, De Napoli L, Orrù S, Pucci P (1997) Identification of the active site nucleophile in the thermostable β-glycosidase from the archaeon *Sulfolobus solfataricus* expressed in *Escherichia coli*. Biochemistry 36:3068–3075

Fukuchi S, Nishikawa K (2001) Protein surface amino acid compositions distinctively differ between thermophilic and mesophilic bacteria. J Mol Biol 309:835–843

Gentile F, Amodeo P, Febbraio F, Picaro F, Motta A, Formisano S, Nucci R (2002) SDS-resistant active and thermostable dimers are obtained from the dissociation of homotetrameric β-glycosidase from hyperthermophilic *Sulfolobus solfataricus* in SDS. J Biol Chem 277:44050–44060

Hendsch ZS, Tidor B (1994) Do salt bridges stabilize proteins? A continuum electrostatic analysis. Protein Sci 3:211–226

Hubbard SJ, Thornton JM (1993) NACCESS computer program. Department of Biochemistry and Molecular Biology, University College London

Jackson M, Mantsch HH (1991) Beware of proteins in DMSO. Biochim Biophys Acta 1078:231–235

Jaenicke R (1996) Stability and folding of ultrastable proteins: eye lens crystallins and enzymes from thermophiles. FASEB J 10:84–92

Jaenicke R, Böhm G (1998) The stability of proteins in extreme environments. Curr Opin Struct Biol 8:738–748

Karshikoff A, Ladestein R (2001) Ion pairs and thermotolerance of proteins from hyperthermophiles. Trends Biochem Sci 26:550–556

Koradi R, Billeter M, Wüthrich K (1996) MOLMOL: a program for display and analysis of macromolecular structures. J Mol Graph 14:51–55

Krimm S, Bandekar J (1986) Vibrational spectroscopy and conformation of peptides, polypeptides, and proteins. Adv Protein Chem 38:181–364

Lo Nostro P, Frantoni L, Ninham BW, Baglioni P (2002) Water absorbency by wool fibers. Hofmeister effect. Biomacromolecules 3:1217–1224

Marqusee S, Sauer RT (1994) Contributions of a hydrogen bond/salt bridge network to the stability of secondary and tertiary structure in repressor. Protein Sci 3:2217–2225

McDonald IK, Thornton JM (1994) Satisfying hydrogen bonding potential in proteins. J Mol Biol 238:777–793

Neagu A, Neagu M, Der A (2001) Fluctuations and Hofmeister effect. Biophys J 81:1285–1294

Nucci R, Moracci M, Vaccaro C, Vespa N, Rossi M (1993) Exo-glucosidase activity and substrate specificity of the β-glycosidase isolated from the extreme thermophile *Sulfolobus solfataricus*. Biotechnol Appl Biochem 19:239–250

Osborne HB, Nabedryk-Viala E (1982) Infrared measurements of peptide hydrogen exchange in rhodopsin. Methods Enzymol 88:676–680

Pace CN (2000) Single surface stabilization. Nat Struct Biol 7:345–346

Paolini S, Tanfani F, Fini C, Bertoli E, Pelosi P (1999) Porcine odorant-binding protein: structural stability and ligand affinities measure by Fourier-transform infrared spectroscopy and fluorescence spectroscopy. Biochim Biophys Acta 1431:179–188

Pedone E, Bartolucci S, Rossi M, Pierfederici FM, Scirè A, Cacciamani T, Tanfani F (2003) Structural and thermal stability analysis of *Escherichia coli* and *Alicyclobacillus acidocaldarius* thioredoxin revealed a molten globule-like state in thermal denaturation pathway of the proteins. An infrared spectroscopic study. Biochem J 373:875–883

Pfeiffer S, Fushman D, Cowburn D (1999) Impact of Cl^- and Na^+ ions on simulated structure and dynamics of βARK1 PH domain. Proteins 35:206–217

Sali D, Bycroft M, Fersht AR (1991) Surface electrostatic interactions contribute little to stability of barnase. J Mol Biol 220:779–788

Strickland EH (1974) Aromatic contribution to circular dichroism spectra of proteins. CRC Crit Rev Biochem 2:113–175

Sun DP, Sauer U, Nicholson H, Matthews BW (1991) Contributions of engineered surface salt bridges to the stability of T4 lysozyme determined by directed mutagenesis. Biochemistry 30:7142–7153

Szilàgyi A, Zavodszky P (2000) Structural differences between mesophilic, moderately thermophilic and extremely thermophilic protein subunits: results of a comprehensive survey. Struct Fold Des 8:493–504

Tanfani F, Kulawiak D, Kossowska E, Purzycka-Preis J, Zydowo MM, Sarkissowa EWE, Wozniak M (1998) Structural-functional relationships in pig heart AMP-deaminase in the presence of ATP, orthophosphate, and phosphatidate bilayers. Mol Genet Metab 65:51–58

Umemura J, Cameron DG, Mantsch HH (1980) A Fourier transform infrared spectroscopic study of the molecular interaction of cholesterol with 1,2-dipalmitoyl-*sn*-glycero-3-phosphocholine. Biochim Biophys Acta 602:32–44

Vogt G, Woell S, Argos P (1997) Protein thermal stability, hydrogen bonds, and Ion pairs. J Mol Biol 269:631–643

Waldburger CD, Schildbach JF, Sauer RT (1995) Are buried salt bridges important for protein stability and conformational specificity? Nat Struct Biol 2:122–128

Weiner PK, Kollman PA (1981) AMBER: assisted model building with energy refinement. A general program for modelling molecules and their interactions. J Comput Chem 2:287–303

Weiner SJ, Kollman PA, Case DA, Chandra Singh U, Ghio C, Alagona G, Profeta S, Weiner PK (1984) A new force field for molecular mechanical simulation of nucleic acids and proteins. J Am Chem Soc 106:765–784

Weiner SJ, Kollman PA, Nguyen DT, Case DA (1986) An all atom force field for simulations of proteins and nucleic acids. J Comput Chem 7:230–252